universität innsbruck

Diode-laser

Alexander Helbok*, Jakob Höck †, Max Koppelstätter‡

April 3, 2024

Comments: Data analysis has been done extremely thoroughly and presented very well. All results look accurate as well. Good job! Pay attention to language in the report as in many places, the language used is not very scientific. Further, you have skipped mentioning certain details in your setup and how you have obtained your results.

Grading:
1. Preparation: 2/2
2. Execution: 1/1
3. Report: 6.7/7
   (i) Introduction and Theory: 2/2
   (ii) Experimental Description: 0.7/1
   (iii) Results and analysis: 2/2
   (iv) Intepretation and Discussion: 2/2

Total - 9.7/10

Abstract

The aim of this report is to characterize a diode-laser. Firstly, the output power of the laser diode is recorded for different input-currents and three different temperatures. This allows us to determine both threshold current and efficiency. We observe the threshold current going up with temperature, whilst the efficiency remains constant. The second part of the experiment includes a Fabry-Perot interferometer, allowing us to study the frequency tuneability of the laser with respect to current and temperature. Overall, frequency decreases with both increasing temperature and current, with current adjustments being the finer ones.

*alexander.helbok@student.uibk.ac.at
†jakob.hoeck@student.uibk.ac.at
‡max.koppelstaetter@student.uibk.ac.at

Contents

0 Introduction

What would a world without laser technology look like? Well, it would look really different than the world we know. From GPS to accurate clocks, lasers are omnipresent in the modern world. But not only technical applications are worth mentioning here; they also play an indispensable role in various physical experiments, shedding light on phenomena ranging from quantum mechanics to material science. In a recent experiment, we delved into the behaviors of a diode laser, a type known for its affordability and compact design.

In this analysis, our focus is twofold. Firstly, we examine the power output of the diode laser as a function of the current applied to it. Through this investigation, we also scrutinized the temperature dependency of the threshold current, providing insight into the intricate relationship between temperature and laser performance. Secondly, we explore the frequency dependency of the laser output. To accomplish this, we employ an optical cavity, which facilitates the measurement of specific frequency branches. This technique not only allows for precise frequency analysis but also enables spectroscopic studies, providing a deeper understanding of the laser's spectral characteristics and potential applications in various fields. Following a brief theoretical overview and an explanation of the applied theory, this report will present and discuss the evaluated data.

1 Theory

In this section, the basic theoretical principles are briefly outlined to provide a better understanding of how the diode laser operates.

1.1 Optical Resonator

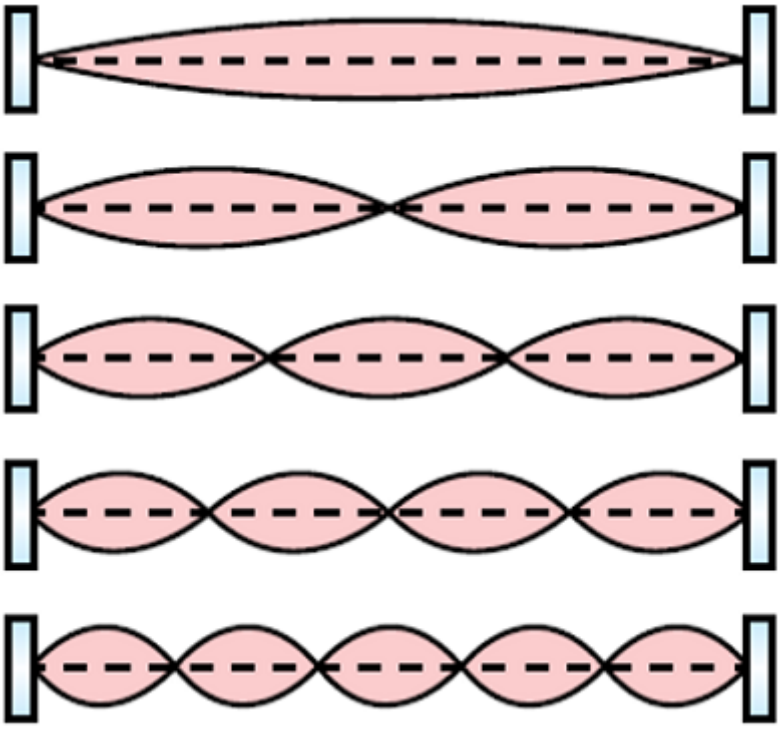

Figure 1: In this figure, it is possible to see the five first possible modes. From [1].

In an optical resonator, two mirrors are set up parallel to each other at a certain distance L. Due to the fact that the electric field has a node at each mirror, only waves with a wavelength λ that is an integer inverse of the half distance between those mirrors can exist as standing waves. So we get the general relation

$$\lambda_n = \frac{2L}{n},$$

where L is the length between the two mirrors. This behavior is shown in Figure 1. It should be noted that the propagation velocity varies depending on the medium, with the refractive index given by the ratio $\eta = c/c_{\mathrm{m}}$, where c is the speed of light in vacuum and c_{m} is the propagation speed in the medium. So with that, it is possible to find the frequencies of the standing waves between the mirrors

$$\nu_n = \frac{c_{\mathrm{m}}}{\lambda_n} = \frac{c}{2\eta L} \cdot n.$$

In this relation, n is an Integer number, η is the refractive index, and L is the length between the mirrors. This relation can be simplified if we define the free spectral range (FSR) as $\mathrm{FSR} = c/(2\eta \cdot L)$. So the relation becomes $\nu = n \cdot \mathrm{FSR}$ (see [2]). An external factor that changes the frequency which the resonator can emit, is temperature. When heated, the entire system expands, resulting in a larger L. This in turn reduces ν. If the mirrors are semi-transparent, monochromatic light can be emitted. Depending on the transmittance, other frequencies can also pass through the mirror and the peaks smooth out (see [3]). This behaviour is shown in Figure 2. To make it clear, to get an more clear peak in the spectrum the mirrors must be more reflective.

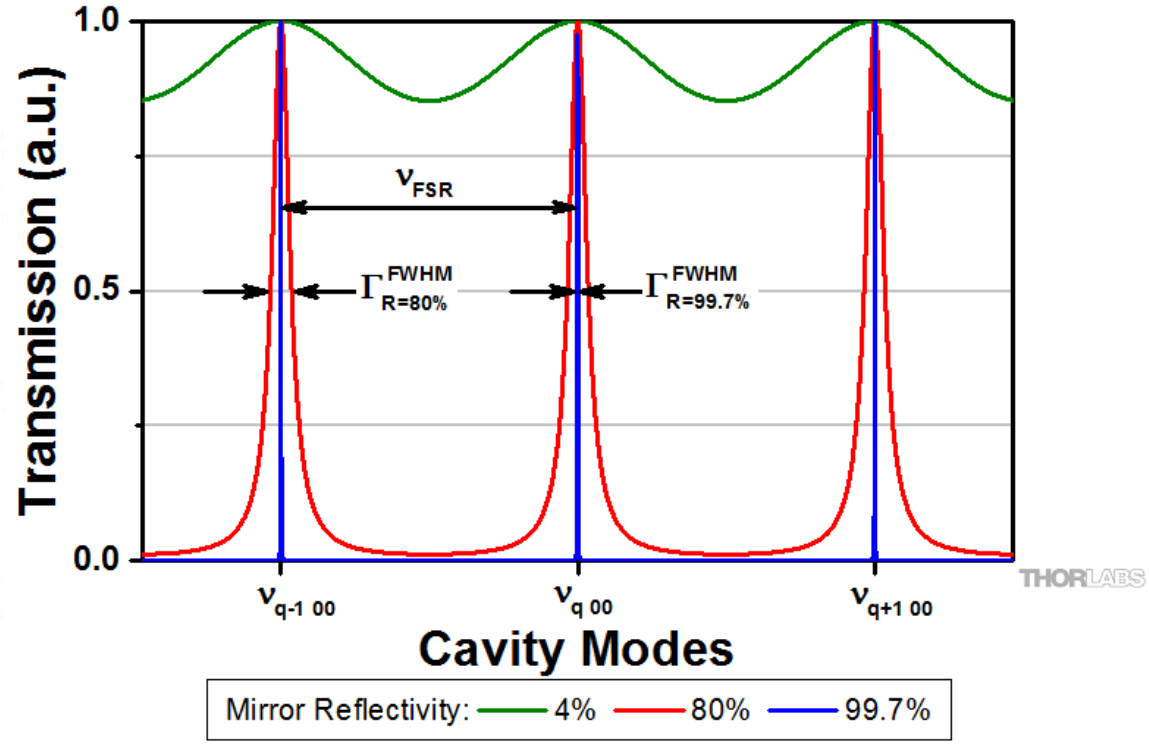

Figure 2: „Mode spectrum of a Fabry-Pérot interferometer for mirror reflectances of 99.7%, 80%, and 4%, illustrated by a blue, red, and green curve, respectively. 99.7% reflectance corresponds to the case for the SA200 series, which has a free spectral range of 1.5 GHz. The 4% reflectance corresponds to a typical "fringing effect" arising from reflections between parallel surfaces on glass plates."From [3].

1.2 Semiconductors

Semiconductors, like conductors and insulators, feature a band structure composed of two key energy bands: the valence band and the conduction band. In contrast to conductors, semiconductors and insulators exhibit a gap between these bands, termed the bandgap, which is narrower in semiconductors. The valence band houses electrons at absolute zero temperature, tightly bound to their atoms and offering minimal electrical conductivity. Above the valence band lies the conduction band, where electrons can move freely upon receiving energy, such as from an electric field or thermal excitation. Consequently, semiconductors share similarities with insulators at zero temperature. The width of the energy gap between the valence and conduction band determines semiconductor conductivity. Insulators possess a wide gap, limiting electron mobility, while conductors feature overlapping bands enabling electron movement. Semiconductors, with their narrower gap, allow electrons to transition from the valence to the conduction band, thereby increasing conductivity under conditions like higher temperatures or through doping with impurities. Doping involves intentionally introducing impurities into a semiconductor, such as phosphorus for n-type doping or boron for p-type doping, which alters the conductivity characteristics by introducing additional charge carriers (either electrons for n-type doping or "holes" for p-type doping) into the semiconductor crystal lattice (see [4]).

1.3 Diode Laser

As already mentioned in the name, this is a diode. A diode is a semiconductor component that conducts electric current in one direction while blocking it in the opposite direction. It consists of a p-doped and an n-doped semiconductor material that are connected to each other at the so-called pn junction. In the forward direction, when positive voltage is applied to the p-doped area and negative voltage to the n-doped area, the diode allows current to flow. In the reverse direction, when the voltage is applied in the opposite polarity, the diode effectively blocks the flow of current. Diodes are used in numerous electronic circuits, including rectifiers, voltage regulators and protection circuits.

The recombination of an electron-hole pair emits a photon. To observe this phenomenon, the semiconductor must be transparent. When n- and p-doped semiconductors come into contact with no external current, the free electrons and holes recombine and create a depletion region at the surface. Upon applying an external current, this depletion region will decrease in size, facilitating spontaneous recombination of electron-hole pairs. Eventually, the depletion region will completely vanish, allowing for the emission of a large number of photons. The current at this point is called threshold current I_{th}. We expect a linear behaviour between photon power P and current above I_{th} and can be represented by following function:

$$P(I) = \eta\,(I - I_{\mathrm{th}})\,. \tag{1}$$

Here, the slope η stands for the efficiency of the diode. Dividing η with the energy one photon carries one can define the differential quantum efficiency, describing the efficiency of electron to photon conversion

$$\eta_d = \eta \frac{e\lambda}{hc},$$

where hc/λ is the ideal energy of a photon and e is the elementary charge of an electron. (see [2]).

These behaviors not only apply to laser diodes but also characterize LEDs (light-emitting diodes). However, the phenomenon of "lasing" specifically occurs in laser diodes. In an LED, light emission results from the spontaneous recombination of electrons and holes across the semiconductor junction,

producing incoherent light. In laser diodes, input current is increased until internal radiation losses become small and spontaneous emission turns into stimulated emission, creating coherent photons. Additionally, laser diodes feature an applied cavity, facilitating the production of monochromatic light, by limiting the allowed frequencies as described in subsection 1.1. The schematic structure can be seen in Figure 3. It can be seen that we enclose the structure of a diode at the ends with mirrors so that the emitted photons are converted directly into monochromatic light. Most of the photons whose wavelength cannot exist in the cavity are absorbed again.

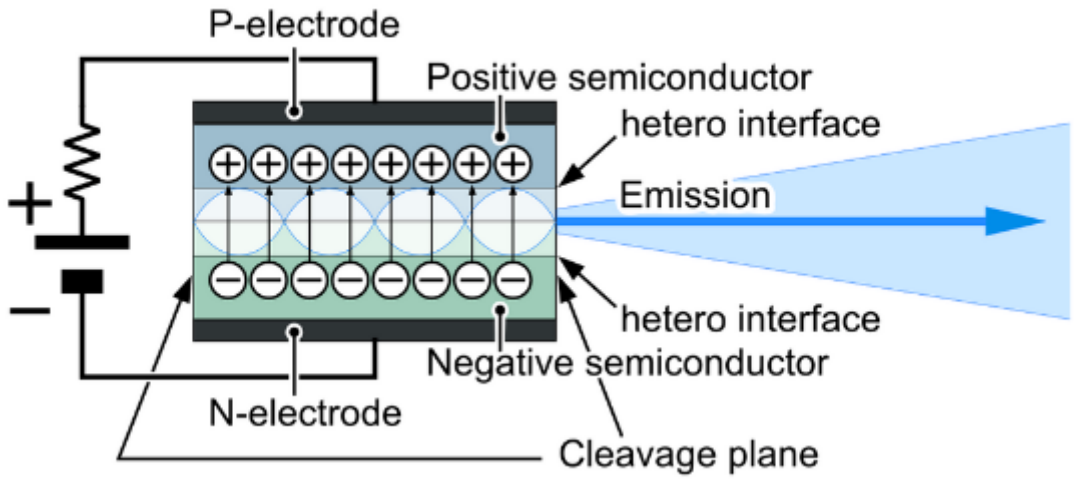

Figure 3: The schematic layout of the laser diode can be seen in this image. The p- and n- doped semiconductors can be seen as well as the location where the cavity mirrors are attached. The direction in which the laser is emitted can also be recognised. From [5]

1.4 Laser modes and mode hopping

As previously outlined, only specific discrete modes are emitted within a cavity. Conversely, an LED emits a Gaussian spectrum. To ascertain the modes of the laser diode, it is necessary to multiply the discrete regions within the cavity by the photon emission signal to derive the actual modes of the laser diode. The product of this behaviour can be seen as an example on a 1 mm cavity in Figure 4.

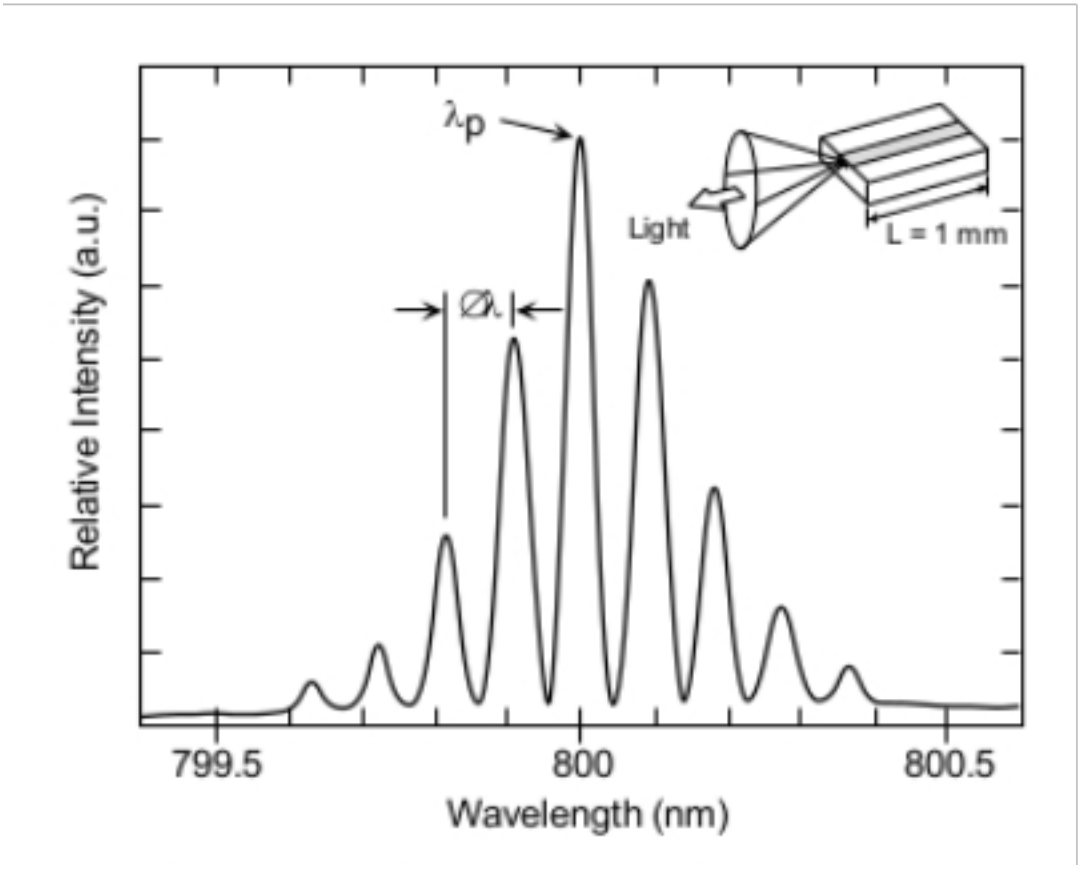

Figure 4: "Typical spectrum of an 1 mm cavity length laser diode operating just above threshold. The peak wavelength of emission (λ_P) is at 800 nm. The separation between adjacent peaks($\varnothing\lambda$) is about 0.09 nm." [6]

If external parameters, such as the temperature of the diode, are altered, the cavity's behavior undergoes a shift, causing the spacing between frequencies to decrease and shift to the left. Consequently, the behavior of the emitted light also alters, albeit prediction of its behavior is nontrivial, since the gain profile of the diode also changes in unknown manners. Consequently, the dominant peak shifts to another, resulting in what is known as mode hopping.

2 Procedure and setup

In this section, the experimental setup and all used components are described. The setup contains a laser diode with implemented temperature regulator. The laser beam gets redirected over two mirrors and enters a Fabry-Perot-Interferometer (FPI). This cavity consists of two parallel mirrors, whereby the rear mirror is moved forwards and backwards by a Piezo-Transducer. The setup is shown in Figure 5.

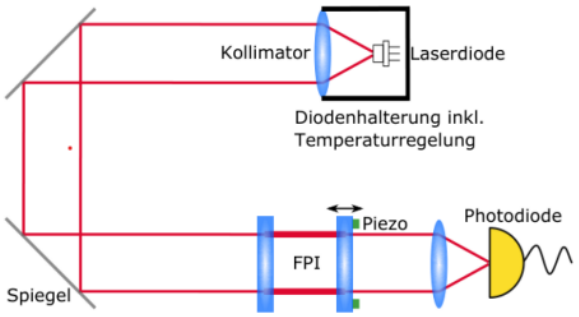

Figure 5: The experimental setup containing the laser diode, two deflecting mirrors, the FPI, with one mirror moved by a Piezo-transducer, and a photodiode afterwards. From [2].

In the first part, the emitted power of the laser beam is detected in dependence of the input-current. This measurement series is done for three different temperatures, 20 °C, 25 °C and 30 °C. For each temperature, the current is varied from 0 mA to 35 mA in 21 steps. At currents below the threshold current we use steps of 1 mA. When lasing starts up, steps of 0.2 mA are used in order to accurately determine the threshold current. Afterwards, bigger steps are used again. For every current, the power is manually read off the powermeter.

In the second part of the experiment, the frequency tuneability is being measured. Therefore, a triangle voltage is inserted at the Piezo-transducer, which is left unchanged during the experiment. The measured signal of the photodiode is saved onto an USB-stick from an oscilloscope connected to the photodiode. To explore the frequency tuneability dependent on current, three series of measurements are done at three temperatures, 20 °C, 25 °C and 30 °C. In each case, the current is varied in 26 steps, starting at each threshold current that resulted from the first part of the experiment. Afterwards, the current is held constant at 35.00(1) mA. Now, the temperature is changed from 20 °C to 30 °C in steps of 1 °C. It does not make sense to use smaller steps, as the screw that works as the temperature regulator does not provide higher resolution.

3 Results

To determine the power characteristics of the laser, the input current was varied at constant temperatures. The temperature is controlled via a knob and the uncertainty is estimated to be 0.2 °C. The current set on the power supply remained fairly stable on the digital display, which is why we chose the uncertainty to be in the last digit of the display (0.01 mA).

The output power of the laser was measured with a power meter accounting for background radiation. Due to some fluctuations the uncertainty was set to 0.1 µW or 0.1 mW, depending on the power meters scale.

In Figure 6 the measured power P is plotted against current I. The measurements were done at different temperatures $T = 20\ °C, 25\ °C$ and 30 °C, denoted by different colors. The uncertainty of the datapoints is of the order of the point size and can therefore not be seen in the plot.

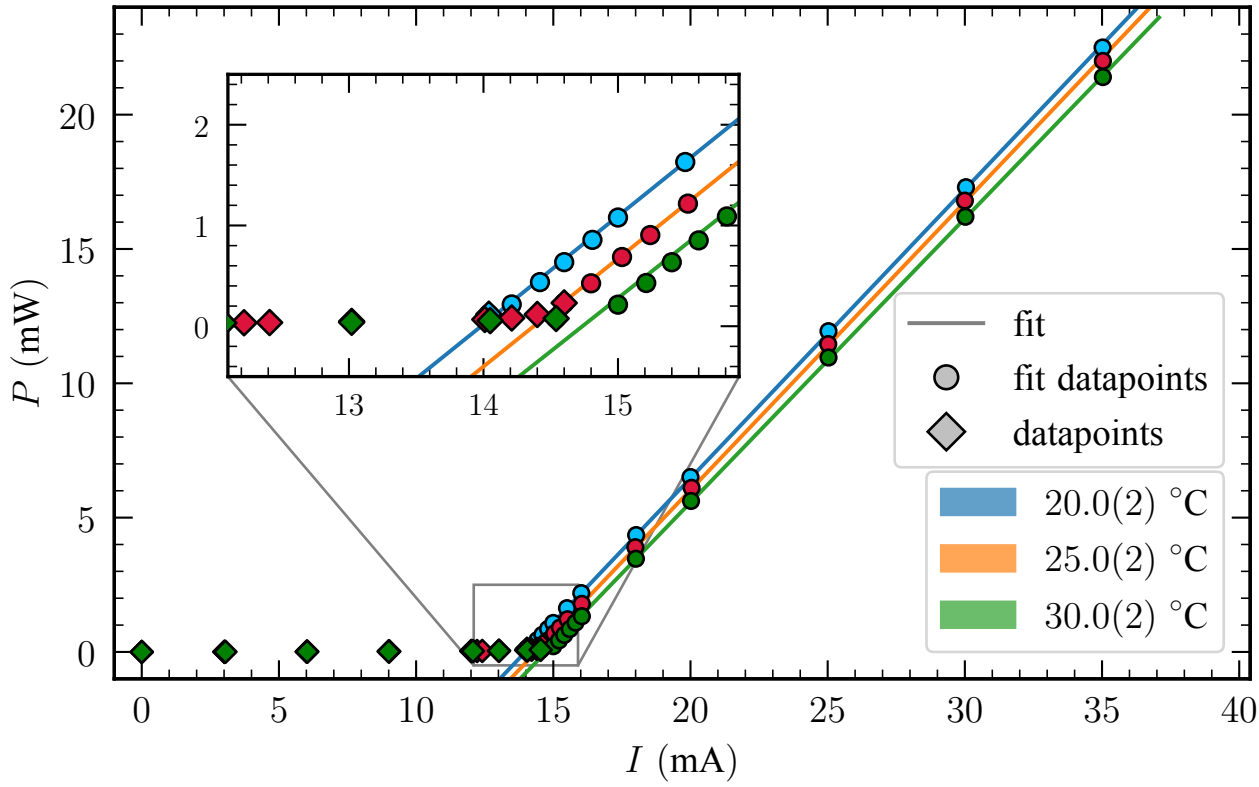

Figure 6: The output power P of the laser is measured for different currents I and temperatures T. Linear functions are fitted to datapoints in the linear regime (circles), while the data not used for fitting are rhombi. The measurements at different temperatures are marked with different colors.

Theory tells us (see subsection 1.3), that below a threshold current I_{th}, the emitted power of the laser comes from spontaneous emission without much increase in power with added current. Above I_{th} lasing starts and the power dependence is linear. Looking at Figure 6 one can clearly see the two regions with I_{th} lying around 14 mA. It is also apparent, that I_{th} moves to higher currents with increasing temperature. To accurately determine the threshold current and the efficiency of the laser we selected datapoints in the linear region and fitted a linear function of the type $P(I) = \eta(I - I_{\text{th}})$. The fitted values for threshold current I_{th}, efficiency η and differential quantum efficiency η_d can be seen in Table 1.

Table 1: Fitted threshold current I_{th}, efficiency η and differential quantum efficiency η_d for three different temperatures.

T in °C	I_{th} in mA	η	η_d
20.0(2)	13.982(14)	1.075(4)	0.581(2)
25.0(2)	14.374(15)	1.072(5)	0.579(3)
30.0(2)	14.73(4)	1.06(1)	0.572(5)

After determining the power characteristics of the laser, the frequency dependence is of importance. To analyze this, we used a setup including a Fabry-Perot Interferomenter (FPI) and an oscilloscope, as described in section 2.

In order to analyze frequencies, we need to convert the time domain measurements from the oscilloscope to frequencies. This can be done assuming $\text{FSR}_{\text{FPI}} = 630$ GHz and using the difference between

adjacent FPI modes as reference length. The differences were calculated by fitting pseudo-voigt functions [7] to isolated and prominent peaks from 10 handpicked datasets.

The raw data can be seen in Figure 7. Here the frequency spectrum from the oscilloscope is plotted against the laser current, whilst colors represent the voltage amplitude of the recorded spectrum. The heatmaps are labelled according to the value (temperature or current) that remained constant over the measurements.

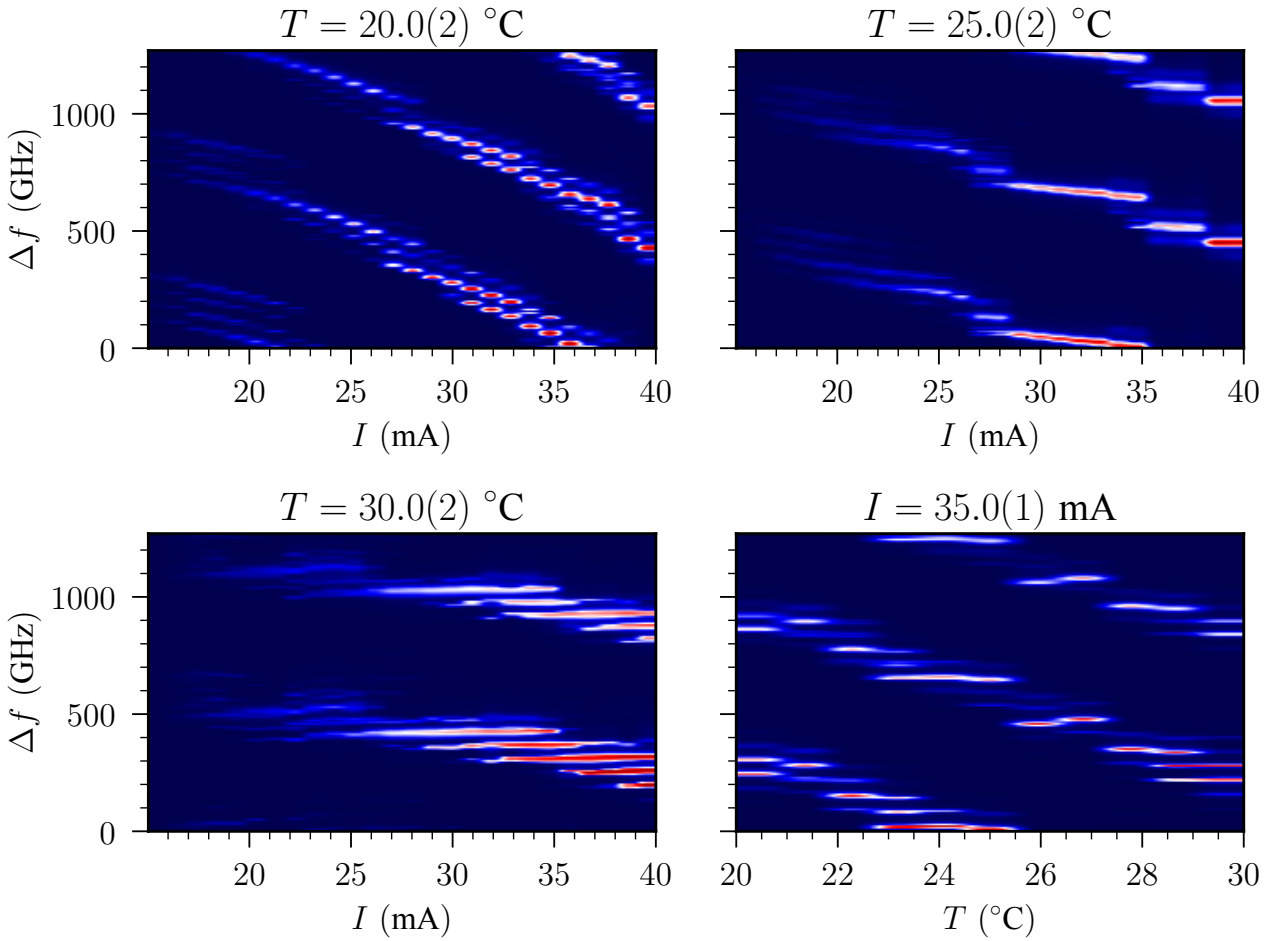

Figure 7: Heatmaps of the frequency spectrum holding one control parameter (temperature or current) constant and varying the other one. The colors are a proxy for the laser power, represent the amplitude of the signal on the oscilloscope.

In Figure 7 one can clearly see jumps between different lasing modes, as described in subsection 1.4. To put numbers on the frequency characteristics of the laser we have to analyze the position and width of the peaks in intensity. We did this by firstly normalizing the data to lie between 0 and 1 using the highest datapoint and then locating peaks that lie above 0.85, since we can have multiple modes with expressed peaks, depending on the gain profile. This value was manually chosen such that we catch prominent overlapping modes without littering the subsequent plots with less important datapoints (we are mainly interested in the dominant mode). Once we have located the peaks used for analysis, we fit a pseudo-voigt function to data withing 25 GHz of the peak. From this we can extract the center of the peak, with the full width at half minimum (FWHM) as chosen uncertainty.

In Figure 8 one can see the relative frequency shift of the laser Δf with respect to input current I, whilst holding the temperature T constant. We chose the first datapoint to be the frequency reference.

We identified datapoints belonging to the same mode by overlaying Figure 8 with the heatmaps from Figure 7 and grouped the data by color. Data not belonging to any major mode are marked white. Additionally we fitted linear functions of the type $f(I) = kf + d$ to every mode (solid lines) and once to all data (dashed line). Both x- and y-error are almost too small to make out in the plot.

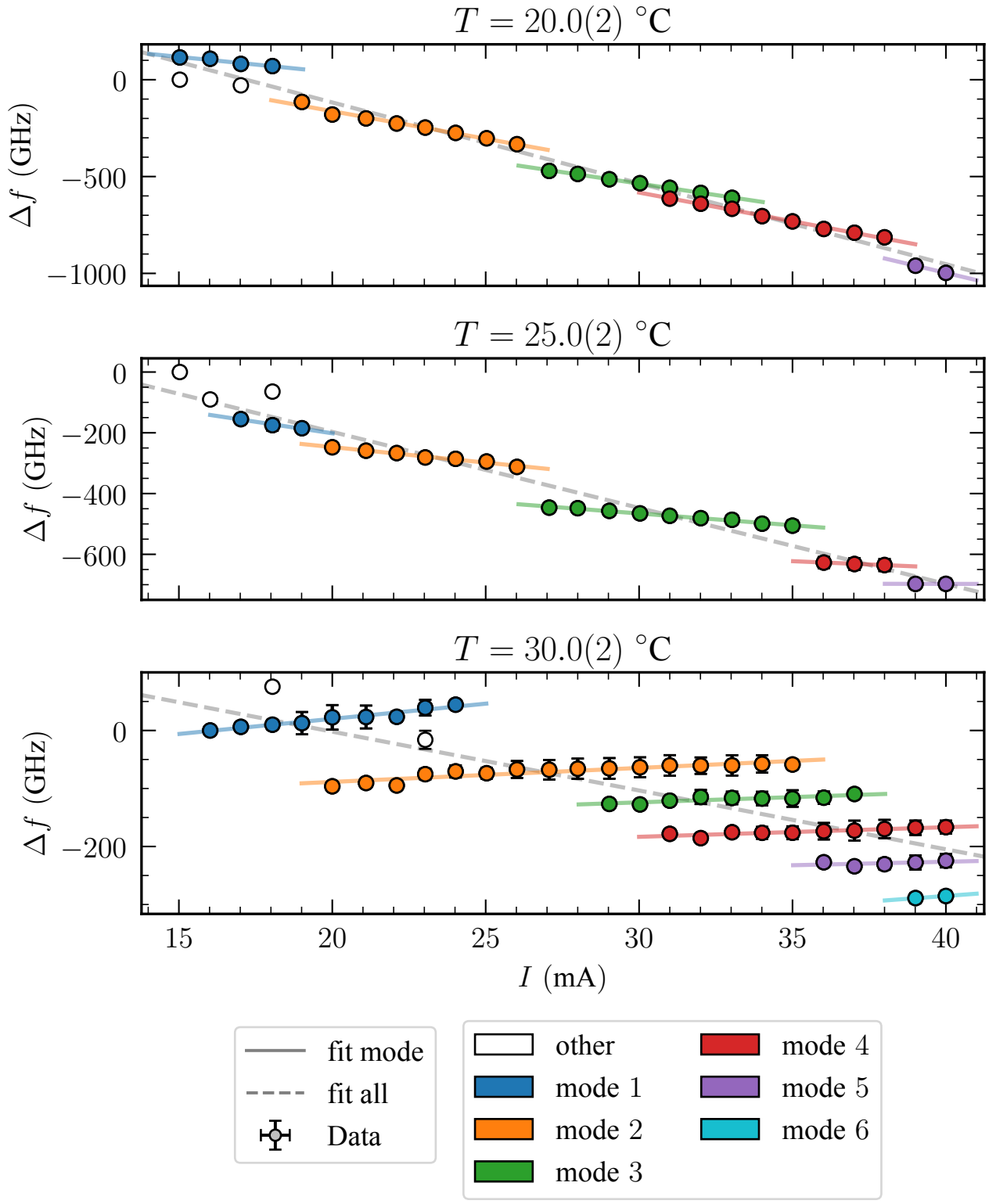

Figure 8: The fitted frequency of intensity peaks, relative to the first datapoint, is plotted for three different temperatures and varying current. The temperature can be seen above the plot. Datapoints lying on different modes were identified and marked by color. Linear function were fitted to the different modes (solid lines) and once to the entire data (dashed line).

The same was done with swapped control parameters, keeping the current constant at $I = 35.00(1)$ mA and varying the temperature in steps of 1 °C. A finer step size could not be realized due to the coarse scale on the laser. Again, the modes were determined by comparing the data with Figure 7, which is of big importance here, since we only have at most three datapoints in the same mode.

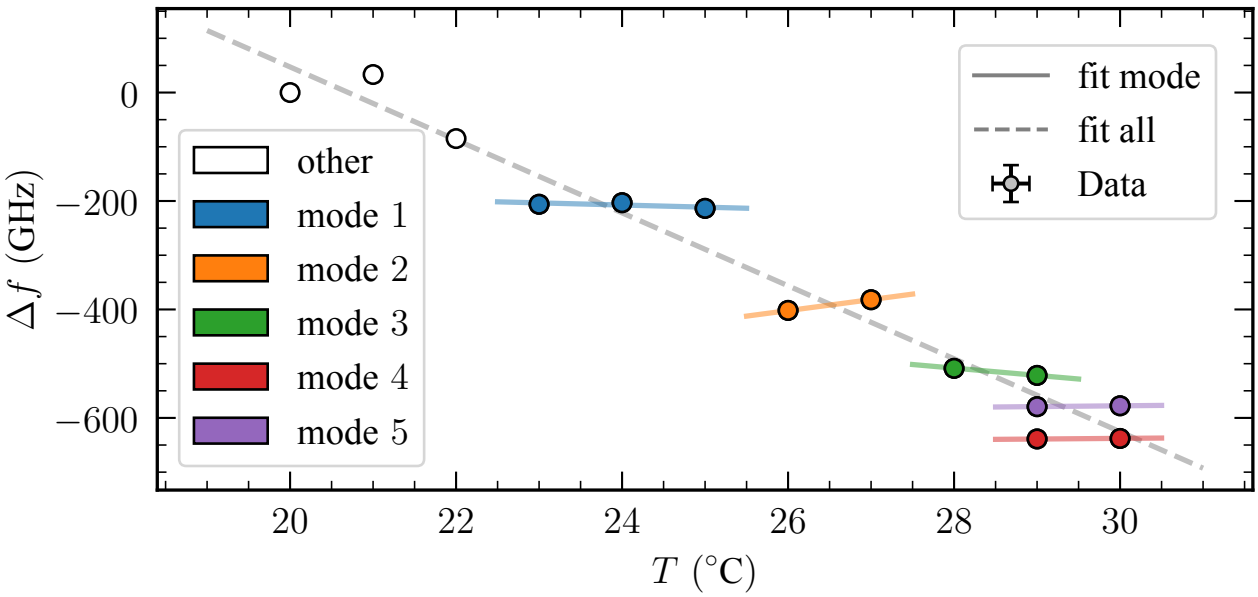

Figure 9: The fitted frequency of intensity peaks, relative to the first datapoint, is plotted at varying temperatures, holding current constant at 35.00(1) mA. Datapoints lying on different modes were identified and marked by color. Linear function were fitted to the different modes (solid lines) and once to the entire data (dashed line).

The determined slopes from all the linear fits can be found in Table 2. Since we fitted functions with two free parameters, fits that were performed on few datapoints should be taken with caution. When dealing with only two datapoints, the uncertainty of the slope is omitted in Table 2, since it can not be defined in a meaningful way.

Table 2: The slopes for all fits seen in Figure 8. Some values have purposely missing uncertainties, since there are no degrees of freedom left in the fits.

	slope of mode fit in GHz/K						
T in °C	1	2	3	4	5	6	all
20.0(2)	−16(5)	−28(2)	−24(2)	−30(1)	−37		−41.8(2)
25.0(2)	−15(7)	−10(2)	−8(2)	−4(13)	0		−27.3(4)
30.0(2)	5(1)	5(1)	2(1)	1(1)	1(3)	4	−10.1(2)
	slope of mode fit in GHz/mA						
I in mA	1	2	3	4	5	6	all
35.00(2)	−3(6)	19.2	−13.0	0.8	1.4		−67.3(6)

Lastly, we will determine the free spectral range (FSR) of the diode. For this we need to measure the distance between adjacent peaks from the same FPI mode. As can be seen in Figure 7 and Figure 8,

the best data for this analysis is with constant temperature at 30 °C, since we have multiple peaks at the same current value. Again, we fitted voigt profiles to the peaks and calculated the difference. We get a mean mode spacing of

$$\mathrm{FSR}_{\mathrm{diode}} = 62(2)\ \mathrm{GHz}.$$

4 Discussion

The measured output power of the laser diode at three different temperatures resulted in a very similar efficiency η and differential quantum efficiency η_d derived from it. This is in perfect agreement with theory. As expected, the threshold current I_{th} is increasing with rising temperatures, due to bigger internal losses at higher temperatures.

When expanding our experimental setup to include a Fabri-Perot interferometer (FPI), we can clearly see the different modes from the FPI, as well as the internal laser modes from the diode. Assuming the FPIs free spectral range to be $\mathrm{FSR}_{\mathrm{FPI}} = 630$ GHz, we can convert the oscilloscopes time domain measurements into frequencies, enabling us to analyze some frequency characteristics of the diode. By analyzing the distance between adjacend intensity peaks, the internal mode spacing of the laser diode was determined to be $\mathrm{FSR}_{\mathrm{diode}} = 62(2)$ GHz.

Furthermore we investigated the impact of temperature and laser current on the frequency. This knowledge allows for accurate tuning of the output frequency. We can clearly see an overall decrease in frequency when increasing both temperature and current, since both increase the optical length of the laser, decreasing the frequency. The exact behaviour however is quite unpredictable, since we are hopping between modes due to a changing gain profile of the laser.

Although both control parameter have the same qualitative effect on frequency, changing current can be done more precisely whilst also having a smaller impact on frequency. Temperature adjustments should therefore be reserved for coarse laser tuning, if at all, whilst current bias is preferable for fine tuning.

References

[1] E. optics. *Laserresonator und Resonatormoden*. Online; Abgerufen am 21. 03. 2024. URL: https://www.edmundoptics.de/knowledge-center/application-notes/lasers/laser-resonator-modes/.

[2] *Practical course experiment 09: Diodelaser*. Universität Innsbruck, Innsbruck, AT: Institut für Experimentalphysik, Dec. 2024.

[3] THORLABS. *Fabry-Perot Interferometer Tutorial*. Online; Abgerufen am 21. 03. 2024. URL: https://www.thorlabs.com/newgrouppage9.cfm?objectgroup_id=9021.

[4] S. Simon. *The Oxford Solid State Basics*. OUP Oxford, 2013. ISBN: 9780199680764. URL: https://books.google.at/books?id=QI8jLeTOBAsC.

[5] Wikipedia. *Laserdiode — Wikipedia, die freie Enzyklopädie*. [Online; Stand 22. März 2024]. 2023. URL: https://de.wikipedia.org/w/index.php?title=Laserdiode&oldid=238703514.

[6] P. Kamran S. Mobarhan. *Determination of Principal Parameter*. Online; Abgerufen am 21. 03. 2024. URL: https://www.laserdiodecontrol.com/laser-diode-parameter-overview.

[7] T. Ida, M. Ando, and H. Toraya. "Extended pseudo-Voigt function for approximating the Voigt profile". In: *Journal of Applied Crystallography* 33.6 (Dec. 2000), pp. 1311–1316. URL: https://doi.org/10.1107/S0021889800010219.

Erklärung

Hiermit versichern wir, dass der vorliegende Bericht selbständig verfasst wurde und alle notwendigen Quellen und Referenzen angegeben sind.

April 3, 2024

Alexander Helbok Date

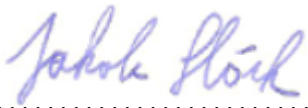

April 3, 2024

Jakob Hugo Höck Date

April 3, 2024

Max Koppelstätter Date